PHYSICAL REVIEW B VOLUME 36, NUMBER 4 1 AUGUST 1987

Bipartition model of ion transport: An outline of new range theory for light ions

Luo Zhengming
Institute of Nuclear Science and Technology, Sichuan University, Chengdu, Sichuan, People's Republic of China
and Institute of Radiation Protection of the Nuclear Industrial Ministry, Tai-yuan, Shanxi, People's Republic of China

Wang Shiming
Institute of Nuclear Science and Technology, Sichuan University, Chengdu, Sichuan, People's Republic of China
(Received 2 December 1986)

Extending the bipartition model of electron transport to the case of light-ion transport, the approximate solution for the light-ion distribution function under the continuously-slowing-down approximation has been developed so as to go a step further in obtaining the light-ion-range profile and other transport quantities [Luo Zhengming, Phys. Rev. B **32**, 812 (1985); **32**, 824 (1985)]. The comparison with existing theories and experiments shows that the new theory not only has the precision which can match with that of the current-transport theory, but is far more flexible in describing the transport process of energetic ions in matter.

I. INTRODUCTION

In recent years the Monte Carlo method has achieved remarkable results in research on ion-beam injection. A vast amount of research has provided important and interesting new results on how to apply the Monte Carlo method for obtaining ion range, energy deposition, reflection coefficients, sputtering yields, etc. In comparison, the standard analytical transport theory, despite its success in calculating the ion range in infinite homogeneous amorphous solids, meets with some essential difficulties when applied to ion transport in solids with boundaries which often occur in practical investigation. Such difficulties are inherent in the moment method. As a result, no effective means can be easily found within the frame of the moment method to overcome them. It seems inevitable for us to try to solve the Boltzmann equation of ion transport at a new angle.[1-3]

A set of studies starting with the present paper is a sample of such an endeavor, in which we shall develop a new theory for ion transport—the bipartition model of ion transport. The theory is actually the direct extension of the bipartition model of electron transport in ion transport. The bipartition model of electron transport has been demonstrated to be successful, with high precision, sufficient flexibility, and high calculating efficiency. The model was introduced almost simultaneously with the range theory developed by Lindhard *et al.*[4-7] It was only recently that the importance of bipartition model to ion transport studies came to be understood. As the multiple-scattering process of electrons in matter has properties very similar to those of the multiple-collision process of ion in solids, it can be expected that this extension will succeed. The basic idea of the ion bipartition model is that the ions entering into the solid are subjected to multiple elastic and inelastic collisions. The former alters the direction and energy of the ions, while the latter generally reduces the energy of ions but does not change the direction greatly. Because of collision, a portion of ions is scattered to the large-angle directions. Their transport behavior is similar to diffusion. We separate these ions from the original ion beam and make them an independent group, called diffusion ions. Since their angular distribution is comparatively closer to isotropy, their transport behavior can be better described in terms of the spherical harmonic method, namely the P_n approximation. The ions that still remain in the original ion beam are necessarily those which only deflect small angles from the original direction, and we call them straightforward ions. Their behavior can be well described in terms of small-angle approximation. The summation of the two groups of ions becomes the general process of ion transport. In order to separate large-angle scattered ions from collided straightforward ions by a suitable means, the partition condition, i.e., the key factor in a bipartition model, will be introduced. The introduction of this condition makes it possible to give an accurate but simple description of charged-particle transport.

The present paper will discuss a comparatively simple case, i.e, the case where light ions are injected into the solid with large atomic weight. This is a very important ion-injection condition. The interaction, for example, between the fusion plasma and the first wall of fusion reactors is one of such conditions. Under this case the Boltzmann equation will be simplified. The paper is divided into five sections: the first is the introduction, the second section studies the various approximations for the Boltzmann equation of ion transport, the third deals with scattering parameters and parameters of stopping power, the fourth gives a bipartition solution of the Boltzmann equation of ion transport under the continuously slowing-down (CSD) approximation, while the fifth is the results and discussions.

II. TRANSPORT EQUATION OF IONS AND ITS VARIOUS APPROXIMATIONS

Although Lindhard *et al.* have done succinct work in introducing a new type of the Boltzmann equation for ion-range distribution, the ordinary ion-transport equation is still used as the starting point of our research because, apart from the final state of ion collision such as ion-range distribution, we are more interested in the actual process of energetic ions in solids. The Boltzmann equation mentioned above that uses the initial energy and initial direction of incident ions as variables is inconvenient for us. In addition, the distribution function we use is not analogous to the ion density distribution. Let $f(\mathbf{r},\mathbf{u},E)$ represent the ion distribution function which is also called the ion differential fluence in angle and energy, then $f(\mathbf{r},\mathbf{u},E)d\mathbf{u}\,dE$ represents the ion fluence at point $\mathbf{r}$, with direction between $\mathbf{u}$ and $\mathbf{u}+d\mathbf{u}$ and with energy between E and $E+dE$. According to the statistical balance principle, we have

$$\mathbf{u}\cdot\nabla f-\frac{\partial f\rho_e}{\partial E}=N\int_{4\pi}d\mathbf{u}'\int_E^{E/(1-\gamma)}dE'\sigma_n(E',E'-E;\mathbf{u}\cdot\mathbf{u}')f(\mathbf{r},\mathbf{u}',E')$$
$$-f(\mathbf{r},\mathbf{u},E)\int_{4\pi}\int_0^{\gamma E}\sigma_n(E,T;\mathbf{u}\cdot\mathbf{u}')dT\,d\mathbf{u}'+S(\mathbf{r},\mathbf{u},E)\ , \tag{1}$$

where N is the number of solid atoms in unit volume. S is an ion-source term. ρ_e is electronic stopping power. $\gamma=4M_1M_2/(M_1+M_2)^2$. M_1 and M_2 are the atomic weight of incident ions and the atomic weight of solid atoms, respectively. From the conservation of energy and momentum, we have

$$\mathbf{u}\cdot\mathbf{u}'=(M_1+M_2)(1-T/E)^{1/2}/2M_1+(M_1-M_2)(1-T/E)^{-1/2}/2M_1\ ; \tag{2}$$

thus the elastic scattering cross section is

$$\sigma_n(E,T;\mathbf{u}\cdot\mathbf{u}')=\sigma_n(E,T)\delta\left[\mathbf{u}\cdot\mathbf{u}'-\frac{M_1+M_2}{2M_1}\left[\frac{E-T}{E}\right]^{1/2}-\frac{M_1-M_2}{2M_1}\left[\frac{E}{E-T}\right]^{1/2}\right]\Big/2\pi\ . \tag{3}$$

Under our condition we have $M_1 \ll M_2$. Consequently, in each collision an ion can transfer only a small portion of energy to the solid atoms or even less energy to electrons in the solid. The slowing-down process may be considered a continuous one, i.e., the CSD approximation (CSDA) is valid. Expanding the collision integral under the condition of small energy transfer, we have a light-ion–transport equation as follows:

$$\mathbf{u}\cdot\nabla f-\frac{\partial}{\partial E}(\rho_e+\rho_n)f=\frac{\partial^2\Omega f}{2\partial E^2}+N\int_{4\pi}d\mathbf{u}'[f(\mathbf{r},\mathbf{u}',E)-f(\mathbf{r},\mathbf{u},E)]\sigma_n(E,\,2E(1-\mathbf{u}'\cdot\mathbf{u})M_1/M_2)+S(\mathbf{r},\mathbf{u},E)\ ,$$
$$\Omega=N\int_0^{\gamma E}T^2\sigma_n(E,T)dT\ . \tag{4}$$

Equation (4) involves energy-loss straggling. The ion-energy-loss straggling is usually small; therefore the term of the collision integral higher than the first order can be neglected. Thus we have the transport equation for light ions,[5]

$$\mathbf{u}\cdot\nabla f-\frac{\partial}{\partial E}(\rho_e+\rho_n)f=N\int_{4\pi}d\mathbf{u}'[f(\mathbf{r},\mathbf{u}',E)-f(\mathbf{r},\mathbf{u},E)]\sigma_n(E,\,2E(1-\mathbf{u}'\cdot\mathbf{u})M_1/M_2)+S(\mathbf{r},\mathbf{u},E)\ . \tag{5}$$

Introducing a scaling transformation

$$t=R_0^{-1}\int_0^E(\rho_e+\rho_n)^{-1}dE'\ , \tag{6}$$

$$\mathbf{y}=\mathbf{r}/R_0\ , \tag{7}$$

then the energy variable can be transformed into relative residual path length t. R_0 is the total path length of the incident ion. Under the scaling transformation the distribution function and ion-source term become

$$f(\mathbf{y},\mathbf{u},t)=f(\mathbf{r},\mathbf{u},E)(\rho_e+\rho_n)R_0\ , \tag{8}$$

$$S(\mathbf{y},\mathbf{u},t)=S(\mathbf{r},\mathbf{u},E)(\rho_e+\rho_n)R_0\ . \tag{9}$$

The CSDA ion-transport equation is

$$\mathbf{u}\cdot\nabla_{\mathbf{y}}f-\frac{\partial f}{\partial t}=NR_0\int_{4\pi}d\mathbf{u}'[f(\mathbf{y},\mathbf{u}',t)-f(\mathbf{y},\mathbf{u},t)]\sigma_n(E(t),\,2E(t)(1-\mathbf{u}\cdot\mathbf{u}')M_1/M_2)+S(\mathbf{y},\mathbf{u},t)\ . \tag{10}$$

III. FITTING PARAMETERS OF ELASTIC SCATTERING CROSS SECTION AND STOPPING POWER

The terms in the ion-transport equation (10) are related to two parameters. One of them is the elastic scattering cross section, and the other, the stopping power of ions. The elastic scattering cross section developed by Lindhard *et al.* has been studied extensively, so the present paper will use newest data of elastic scattering cross section.[8–10] For ease of calculation, the power function approximation of the cross section formula has been used. The parameters λ and m_λ used in the approximation will be determined by means of least-squares (LS) fitting:

$$\delta \int_{\delta E_0}^{E_0} \{3.35z^{-0.233}[1+(6.7z^{0.767})^{0.445}]^{-2.25} - \lambda z^{-m_\lambda}\}^2 dE = 0 , \quad (11)$$

$$z = E_0 E (M_2/M_1)(a/2Z_1Z_2e^2)^2 , \quad (11')$$

where

$$a = 0.8853(Z_1^{2/3}+Z_2^{2/3})^{-1/2} a_0 .$$

a_0 is the Bohr radius. $\delta E_0 = 0.001 E_0$. For the ion stopping power the Ziegler-Anderson table may be used for proton and helium ions.[11] The stopping power of other ions can be found in Refs. 12 and 13. From the stopping power it is easy to obtain the relation between the average path length and energy of ions. The total stopping power is

$$\rho_t = \rho_e + \rho_n , \quad (12)$$

$$\rho_n = \frac{N\pi a^2[2M_1M_2/(M_1+M_2)^2]E \ln(1+\epsilon)}{(\epsilon^2+0.1072\epsilon^{1.3754})} , \quad (12')$$

$$\epsilon = 32.53 M_2 E/[Z_1Z_2(M_1+M_2)(Z_1^{2/3}+Z_2^{2/3})^{1/2}] , \quad (12'')$$

where ρ_n is nuclear stopping power. The path length of ions of energy E is

$$R(E) = \int_0^E dE'/\rho_t(E') . \quad (6')$$

We assume that the fitted formula of the energy path length is

$$E/E_0 = [R(E)/R(E_0)]^\nu = t^\nu , \quad (13)$$

where t is the relative residual path length. By using LS fitting, we have

$$\delta \int_{\delta E_0}^{E_0} (E/E_0 - t^\nu)^2 dE = 0 . \quad (13')$$

Thus the parameter ν can be determined.

IV. BIPARTITION SOLUTION OF THE CSDA EQUATION OF ION TRANSPORT

A. Range distribution of ions in an infinite homogeneous medium

Now we are to discuss a most commonly seen problem of ion transport. An ion beam of energy E_0 is normally incident on the right half of a semi-infinite solid. Let us suppose that the left half-space is composed of a matter identical with that of the solid. Later we shall investigate the case when the left half-space is vacuum. That is a case very often seen in the ion injection. We set up an X axis along the inner normal line direction of the surface. By so doing the ion-transport equation under the CSDA is

$$-\frac{\partial f}{\partial t} + \mu \frac{\partial f}{\partial x} = K t^{-2m_\lambda \nu} \int_{4\pi} d\mathbf{u}'[f(x,\mu',t) - f(x,\mu,t)] \times (1-\mathbf{u}\cdot\mathbf{u}')^{-m_\lambda - 1} + \delta(x)\delta(1-t)\delta(1-\mu)/2\pi , \quad (14)$$

$$K = N\lambda 2^{m_\lambda} a^2 (Z_1Z_2e^2/a)^{2m_\lambda} R_0 / 4E_0^{2m_\lambda} . \quad (15)$$

μ is the cosine of the angle between the direction of ions and the X axis. According to the bipartition model the distribution function $f(x,\mu,t)$ is divided into two parts:

$$f(x,\mu,t) = f_s(x,\mu,t) + f_d(x,\mu,t) . \quad (16)$$

f_s and f_d satisfy the following equations, respectively:

$$-\frac{\partial f_s}{\partial t} + \mu \frac{\partial f_s}{\partial x} = K t^{-2m_\lambda \nu} \int_{4\pi} d\mathbf{u}'[f_s(x,\mu',t) - f_s(x,\mu,t)] \times (1-\mathbf{u}'\cdot\mathbf{u})^{-m_\lambda - 1} - S_d + \delta(x)\delta(1-t)\delta(1-\mu)/2\pi , \quad (17)$$

$$-\frac{\partial f_d}{\partial t} + \mu \frac{\partial f_d}{\partial x} = K t^{-2m_\lambda \nu} \int_{4\pi} d\mathbf{u}'[f_d(x,\mu',t) - f_d(x,\mu,t)] \times (1-\mathbf{u}'\cdot\mathbf{u})^{-m_\lambda - 1} + S_d . \quad (18)$$

Physically, the collision term represents a scattering source. According to the bipartition model we deduct the large-angle scattering source from the collision term in the straightforward ion-transport equation (17) by means of subtracting $S_d(x,\mu,t)$. Consequently, the scattering process generating large-angle ions no longer exists in the straightforward ion-transport equation. Hence its distribution function should describe the transport of small-angle ions only.

B. Partition condition and diffusion ion source

In order to remove large-angle ions from the straightforward ion group and bring them into the diffusion ion group, the following partition condition has been introduced:

$$S_d(x,\mu_i,t) = C_f(x,\mu_i,t) = K t^{-2m_\lambda \nu} \int_{4\pi} d\mathbf{u}'[f_s(x,\mu',t) - f_s(x,\mu_i,t)] \times (1-\mathbf{u}'\cdot\mathbf{u}_i)^{-m_\lambda - 1} , \quad i = 0,1,\ldots,m . \quad (19)$$

The condition shows that all the large-angle scattered ions in a straightforward ion group are regarded as the secondary diffusion ion source S_d. To determine the intensity of this diffusion source, we require that the intensity of the diffusion source comprising the first $m+1$ spherical harmonic components at the $m+1$ large-angle directions be exactly equal to the values of collision integral at the same directions. Expanding the distribution function into a Legendre polynomial series, we have

$$f_s=\sum_{l=0}^{\infty}(2l+1)P_l(\mu)A_l(x,t)/4\pi \ , \tag{20}$$

$$f_d=\sum_{l=0}^{\infty}(2l+1)P_l(\mu)N_l(x,t)/4\pi \ , \tag{21}$$

$$S_d=\sum_{l=0}^{m}\frac{2l+1}{4\pi}P_l(\mu)S_l(x,t) \ . \tag{22}$$

Thus, the collision integral is

$$C_f=-K(E_0/E)^{2m_\lambda}\sum_{l=0}^{\infty}\frac{2l+1}{4\pi}\eta_l P_l(\mu)A_l(x,t) \ , \tag{23}$$

$$\eta_l=2\pi\int_{-1}^{1}[1-P_l(\mu)](1-\mu)^{-1-m_\lambda}d\mu \ . \tag{24}$$

For η_l, we have the following recurrent formula:

$$(l+1-m_\lambda)\eta_{l+1}-(l+1+m_\lambda)\eta_l-4\pi 2^{-m_\lambda}=0, \quad \eta_0=0 \ . \tag{25}$$

In the Appendix we shall give a proof of the formula (25). The partition condition becomes

$$-Kt^{-2m_\lambda v}\sum_{l=0}^{\infty}\frac{2l+1}{4\pi}\eta_l P_l(\mu_i)A_l(x,t) =\sum_{l=0}^{m}\frac{2l+1}{4\pi}P_l(\mu_i)S_l(x,t) \ . \tag{26}$$

Therefore,

$$S_l(x,t)=-Kt^{-2m_\lambda v}\eta_l A_l(x,t) -\sum_{l'=m+1}^{\infty}Kt^{-2m_\lambda v}\eta_{l'}D_{ll'}A_{l'}(x,t) \ . \tag{27}$$

By definition, the bipartition coefficient $D_{ll'}$ is $(2l'+1)\Delta_{ll'}/(2l+1)\Delta$, where

$$\Delta=\begin{vmatrix} 1 & \mu_0 \cdots P_{l-1}(\mu_0) & P_l(\mu_0)\cdots P_m(\mu_0)\\ 1 & \mu_1 \cdots P_{l-1}(\mu_1) & P_l(\mu_1)\cdots P_m(\mu_1)\\ \vdots & & \vdots\\ \vdots & & \vdots\\ 1 & \mu_m \cdots P_{l-1}(\mu_m) & P_l(\mu_m)\cdots P_m(\mu_m)\end{vmatrix}, \quad \Delta_{ll'}=\begin{vmatrix} 1 & \mu_0 \cdots P_{l-1}(\mu_0) & P_{l'}(\mu_0)\cdots P_m(\mu_0)\\ 1 & \mu_1 \cdots P_{l-1}(\mu_1) & P_{l'}(\mu_1)\cdots P_m(\mu_1)\\ \vdots & & \vdots\\ \vdots & & \vdots\\ 1 & \mu_m \cdots P_{l-1}(\mu_m) & P_{l'}(\mu_m)\cdots P_m(\mu_m)\end{vmatrix} \ . \tag{28}$$

C. Straightforward ion group

As the large-angle ions being generated due to elastic collision have been eliminated from the straightforward ion group, only the ions that deflect from the incident direction less than a given smallest angle θ_m can still remain in the straightforward ion group. The θ_m is the smallest angle in the $m+1$ large-angle directions. Since θ_m is generally small, the small-angle property of straightforward ions can be held. Now we may use the small-angle approximation to solve Eq. (17). The so-called small-angle approximation is to substitute $\mu_a(\partial f_s/\partial x)$ for $\mu(\partial f_s/\partial x)$ in Eq. (17),

$$-\frac{\partial f_s}{\partial t}+\mu_a\frac{\partial f_s}{\partial x}=-Kt^{-2m_\lambda v}\sum_{l=0}^{\infty}\frac{2l+1}{4\pi}\eta_l P_l(\mu)A_l(x,t)-S_d+\delta(x)\delta(1-\mu)\delta(1-t)/2\pi \ , \tag{29}$$

where μ_a is the average direction cosine of straightforward ion group. This approximation is reasonable, because $\mu-\mu_a \ll \mu$ for $\mu\approx 1$. The main advantage of this approximation is to remove the coupling between A_l, the angular spherical harmonic moment of the straightforward ion distribution function. By definition, the average direction cosine is

$$\mu_a=\frac{\int_0^1\int_{-1}^{1}\mu f_s(x,\mu,t)dx\,d\mu}{\int_0^1\int_{-1}^{1}f_s(x,\mu,t)dx\,d\mu} \ . \tag{30}$$

Thus we have

$$-\frac{\partial A_l}{\partial t}+\mu_a\frac{\partial A_l}{\partial x}=\begin{cases}\sum_{l'=m+1}^{\infty}Kt^{-2m_\lambda v}\eta_{l'}D_{ll'}A_{l'}(x,t)+\delta(x)\delta(1-t), & l\le m \quad (31)\\ -Kt^{-2m_\lambda v}\eta_l A_l(x,t)+\delta(x)\delta(1-t), & l>m \ . \quad (32)\end{cases}$$

Introducing the Fourier transformation,

$$B_l(p,t)=\int_{-\infty}^{\infty} A_l(x,t)e^{ipx}dx\,, \quad A_l(x,t)=\frac{1}{2\pi}\int_{-\infty}^{\infty} B_l(p,t)e^{-ipx}dp\ . \tag{33}$$

For $l>m$, we have

$$\frac{dB_l}{dt}+i\mu_a(t)pB_l=Kt^{-2m_\lambda\nu}\eta_l B_l-\delta(1-t)\ , \tag{34}$$

$$B_l(p,t)=\exp\left[-\int_t^1[Kt'^{-2m_\lambda\nu}\eta_l-i\mu_a(t')p]dt'\right]\ , \tag{35}$$

$$A_l(x,t)=\delta\left[x-\int_t^1\mu_a(t')dt'\right]\exp[-K\eta_l(1-t^{1-2m_\lambda\nu})/(1-2m_\lambda\nu)]\ . \tag{36}$$

For $l\leq m$, we have

$$-\frac{\partial A_l}{\partial t}+\mu_a(t)\frac{\partial A_l}{\partial x}=-\sum_{l'=m+1}^{\infty}D_{ll'}\left[-\frac{\partial A_{l'}}{\partial t}+\mu_a\frac{\partial A_{l'}}{\partial x}-\delta(1-t)\delta(x)\right]+\delta(1-t)\delta(x)\ . \tag{37}$$

Let $\gamma_l=\sum_{l'=m+1}^{\infty}D_{ll'}$, i.e.,

$$\gamma_l=\frac{1}{(2l+1)\Delta}\begin{vmatrix} 1 & \mu_0\cdots & \sum_{l'=m+1}^{\infty}(2l'+1)P_{l'}(\mu_0) & P_{l+1}(\mu_0)\cdots P_m(\mu_0)\\ 1 & \mu_1\cdots & \sum_{l'=m+1}^{\infty}(2l'+1)P_{l'}(\mu_1) & P_{l+1}(\mu_1)\cdots P_m(\mu_1)\\ \vdots & & & \vdots\\ 1 & \mu_m\cdots & \sum_{l'=m+1}^{\infty}(2l'+1)P_{l'}(\mu_m) & P_{l+1}(\mu_m)\cdots P_m(\mu_m)\end{vmatrix}\ . \tag{38}$$

Using the following formula,

$$\delta(\mu-\mu_i)=\sum_{l=0}^{\infty}(l+\tfrac{1}{2})P_l(\mu)P_l(\mu_i)\ . \tag{39}$$

For $\mu=1$, we have

$$\sum_{l'=m+1}^{\infty}(l'+\tfrac{1}{2})P_{l'}(\mu_i)=-\sum_{l'=0}^{m}(l'+\tfrac{1}{2})P_{l'}(\mu_i)\ . \tag{40}$$

Therefore,

$$\gamma_l=-1\ . \tag{41}$$

Introducing the following Z function, its definition is

$$Z_l=A_l+\sum_{l'=m+1}^{\infty}D_{ll'}A_{l'}\ . \tag{42}$$

Thus, we have

$$\begin{gathered}-\frac{\partial Z_l}{\partial t}+\mu_a\frac{\partial Z_l}{\partial x}=0\ ,\\ Z_l(x,t)=0\ \ \text{when}\ t=1\ ,\\ Z_l(x,t)=0\ \ \text{at}\ x=0\ \text{and}\ x=1\ .\end{gathered} \tag{43}$$

Equation (43) has only a zero solution, then

$$\begin{aligned}A_l(x,t)&=-\sum_{l'=m+1}^{\infty}D_{ll'}A_{l'}(x,t)\\ &=\alpha_l(t)\delta\left[x-\int_t^1\mu_a(t')dt'\right]\ ,\end{aligned} \tag{44}$$

$$\alpha_l(t)=-\sum_{l'=m+1}^{\infty}D_{ll'}\exp\left[\frac{-K\eta_{l'}(1-t^{1-2m_\lambda\nu})}{1-2m_\lambda\nu}\right]\ . \tag{45}$$

Correspondingly, the diffusion ion source is

$$\begin{aligned}S_l(x,t)=\delta&\left[x-\int_t^1\mu_a dt'\right]\\ &\times\left[-Kt^{-2m_\lambda\nu}\eta_l\alpha_l-\sum_{l'=m+1}Kt^{-2m_\lambda\nu}\eta_{l'}D_{ll'}\alpha_{l'}\right]\ ,\\ &\qquad l=0,1,\ldots,m\ .\end{aligned} \tag{46}$$

D. Diffusion ion group

Having calculated the diffusion ion source, it is possible to calculate the distribution function of diffusion ions. Since the angular distribution of diffusion ions is comparatively isotropic, its spherical harmonic moments cannot be decoupled. The cutting-off method is commonly used to decouple it forcibly, that is, we implement the P_n approximation. The so-called P_n approximation is to assume $N_l(x,t)=0$ if $l>n$. Thus we have the following set of hyperbolic partial-differential equations,

$$-\frac{\partial N_l}{\partial t}+\frac{1}{2l+1}\left[(l+1)\frac{\partial N_{l+1}}{\partial x}+l\frac{\partial N_{l-1}}{\partial x}\right]=-K\eta_l t^{-2m_\lambda\nu}N_l+S_l,\quad l=0,1,\ldots,n\ . \tag{47}$$

This set of equations may have analytical solutions under special conditions, but to treat more complex problems, the numerical method is more desirable. When the numerical method is used to solve the set of equations, care should be taken with the stability of the discrete scheme. In the present work the Lax-Wendroff scheme with second-order precision has been used. This scheme has good stability as well as rather high accuracy.[14] For the sake of convenience the set of the equations is often rewritten into a symmetrical form. The following transformation is therefore introduced:

$$M_l(x,t)=(2l+1)^{1/2}N_l(x,t)\ , \tag{48}$$

$$-\frac{\partial M_l}{\partial t}=-\frac{l+1}{\sqrt{(2l+1)(2l+3)}}\frac{\partial M_{l+1}}{\partial x}-\frac{l}{\sqrt{(2l+1)(2l-1)}}\frac{\partial M_{l-1}}{\partial x}-K\eta_l t^{-2m_\lambda v}M_l+(2l+1)^{1/2}S_l,\quad l=0,1,\ldots,n\ . \tag{47'}$$

Such a symmetrical form is advantageous to using Lax-Wendroff scheme.

E. The boundary condition for the semi-infinite medium

As mentioned above, that is often the case with the incidence of ions on the surface of semi-infinite solid. Although, within the frame of moment method, some researchers have made efforts to evaluate the influence of boundary on ion transport, such efforts do not seem quite successful.[15,16] We shall account for the condition for the bipartition theory being applied to the semi-infinite surface of solid. As the left half-space is vacuum, excepting the incident ions, only the ions reflected from the solid surface to the left-hand-side vacuum may exist on the boundary $x=0$. Therefore, the boundary condition on the surface $x=0$ should be as follows:

$$f_d(0,\mu,t)=0,\quad \mu\geqq 0\ . \tag{49}$$

Although the condition (49) is exact, within the finite series of the P_n approximation it cannot be totally and exactly satisfied for determining the distribution function of diffusion ions. Based on it, Mark and Marshak proposed two important types of boundary conditions, respectively, i.e., the Mark condition and the Marshak condition.[17,18] The Mark condition is

$$f_d(0,\mu_i,t)=0,\quad P_{n+1}(\mu_i)=0,\quad \mu_i\geqq 0\ ,\quad i=1,2,\ldots,(n+1)/2\ . \tag{50}$$

Equation (50) treats the left-hand-side vacuum as blackbody, i.e., the ions leaving the solid surface no longer return to the solid. The Marshak condition is

$$\int_0^1 f_d(0,\mu,t)\mu^{2k-1}d\mu=0,\quad k=1,2,\ldots,(n+1)/2\ . \tag{51}$$

Its merit is to ensure that no diffusion ion current is incident upon the solid surface from the vacuum. Generally, when $n>5$, the Mark condition is better than the Marshak condition. Therefore, the Mark condition is used in our computation.

As far as the calculation of the hyperbolic equation (48) in the step-by-step method is concerned, such boundary conditions are not sufficient for determining the $n+1$ spherical harmonic moments $N_l(x,t)$. Therefore some additional conditions should be given. Actually we have the additional condition as follows:

$$\frac{\partial f_d}{\partial t}=\mu_i\frac{\partial f_d}{\partial x}+Kt^{-2m_\lambda v}\sum_{l=0}^{n}(2l+1)\eta_l P_l(\mu_i)N_l(0,t)/4\pi\ ,\quad P_{n+1}(\mu_i)=0,\quad \mu_i<0,\quad i=(n+3)/2,\ldots,n+1\ . \tag{52}$$

Thus, the $n+1$ boundary conditions altogether can determine the values of the $n+1$ spherical harmonic moments on the surface. The step-by-step computation is made close in this way. Because the above-mentioned boundary conditions are introduced, the bipartition model of ion transport may easily be extended to dealing with the complex problems concerning ion transport in multilayer.

V. COMPUTATIONAL RESULTS

On the basis of the above-mentioned bipartition model of ion transport we have worked out a new program of ion transport, BIMIT-CSDA. This program can compute the light-ion–range distribution, the energy deposition, the radiation damage, the reflection coefficients, and so on under the condition that the ions of lower dose are injected into an infinite or semi-infinite solid or multilayer. Some typical results will be given below and compared with experimental data. More extensive results will be presented in another paper.[19]

A. The range distribution of light ions

The ion-range distribution $R(x)$ is actually the distribution of ion flux in solid when the energy of ions is near zero. Because of divergence of the scattering cross section when $E=0$, it is difficult to calculate the flux of ions with zero energy. However, considering the fact that it is due to the enlargement of scattering cross section that the transport of low-energy ions becomes local, there is no notable difference between the ion-range distribution when energy is near zero and the ion-range distribution when energy is zero. Hence we use $N_0(x,\ t=0.01)$ to represent $R(x)$. Obviously, $N_0(x,t)$ satisfies the conservation of particle number, and in fact we have

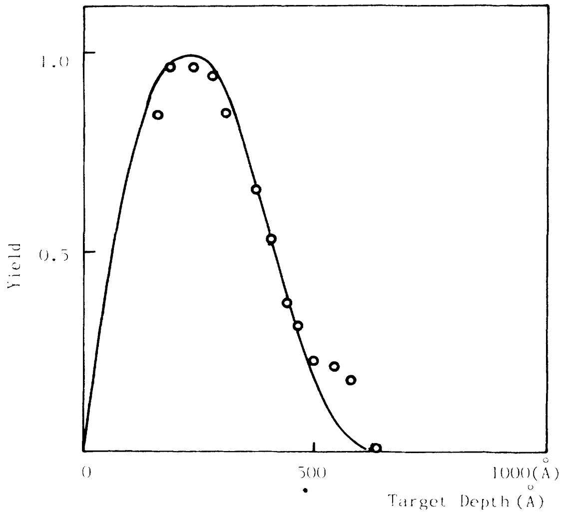

FIG. 1. Hydrogen profile implanted at 1 keV. The solid line is our computational results. ○ is the result measured by Demond *et al.* (Ref. 20).

$$-\frac{\partial N_0}{\partial t}+\frac{\partial N_1}{\partial x}=\delta(1-t)\delta(x)\ . \tag{53}$$

Integrating Eq. (53), we have

$$n_0(t)=\int_{-\infty}^{\infty} N_0(x,t)dx=1\ . \tag{54}$$

For semi-infinite solid, we have

$$n_0=\int_0^{\infty} N_0(x,0)dx\ , \tag{55}$$

$$R_n=-\int_0^1 N_1(0,t)dt\ , \tag{56}$$

$$n_0+R_n=1\ . \tag{57}$$

Equation (57) means that the particle number in the right half-space is equal to the total number of incident particles minus the number of ions reflected from the surface. That is exactly what the conservation law of particle number needs. Figures 1–3 give the range distributions of H^+ ions of 1 and 20 keV in Si. From these results and the corresponding experimental data it may be observed that the bipartition model gives satisfactory results.[20–23]

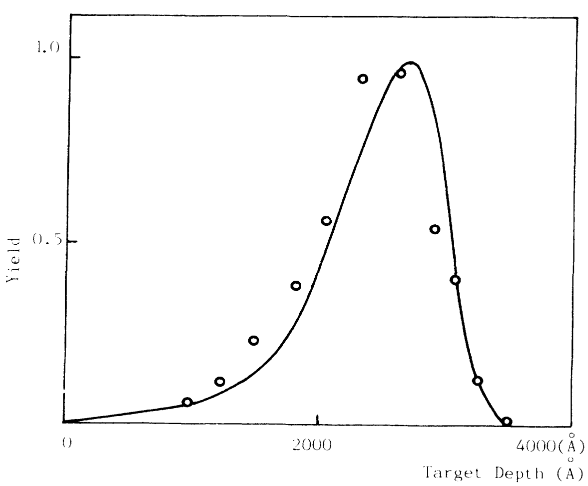

FIG. 2. Hydrogen profile implanted at 20 keV. The solid line is our result. ○ is the result measured by Demond *et al.* (Ref. 20).

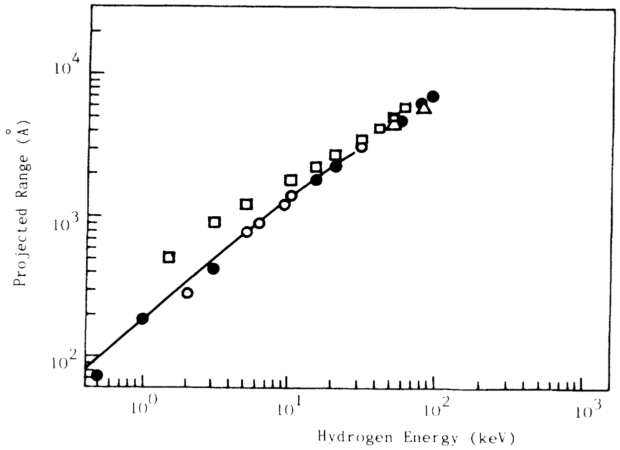

FIG. 3. Mean projected range as a function of ion energy. —— is our result. ○,● represent the data of Demond *et al.*; ■, Marcinkowski *et al.* (Ref. 23); □, Ligeon and Guivarc'h (Ref. 22); △, Chu *et al.* (Ref. 21).

B. The reflection of ions from a surface of solid

The research in the reflection of ions from a surface of solid is essential for the understanding interaction between ions and surface. The most important parameters describing reflection are numerical reflection coefficients and energy reflection coefficients, and next are the angular distribution and the energy spectrum of reflected particles. By definition, the former two parameters R_n, R_e are as follows:

$$R_n=-\int_0^1 N_1(0,t)dt\ , \tag{58}$$

$$R_e=-\int_0^1 N_1(0,t)E(t)dt\ . \tag{59}$$

It is easy to evaluate these transport quantities using the bipartition model. We have calculated the reflection coefficients for hydrogen ions that are normally incident into gold. The energy interval of ions is from 0.01 keV to 1 MeV. This energy interval is one that concerns nuclear-fusion and nuclear-analysis techniques. Figure 4 gives the number reflection coefficients of 0.1–20 keV hydrogen ions being incident upon a gold target. At the same time it gives the experimental data and the Monte Carlo computational results as well. From Fig. 4 it may be seen that the computational results based on the bipartition model agree with the experimental results in a wider energy interval.[24–29]

C. Computational efficiency

As stated above, we have already shown that the bipartition model is characterized by its high precision and sufficient flexibility. Here another important merit of the model is mentioned, i.e., it needs using only far less storage and central-processing-unit (CPU) time of com-

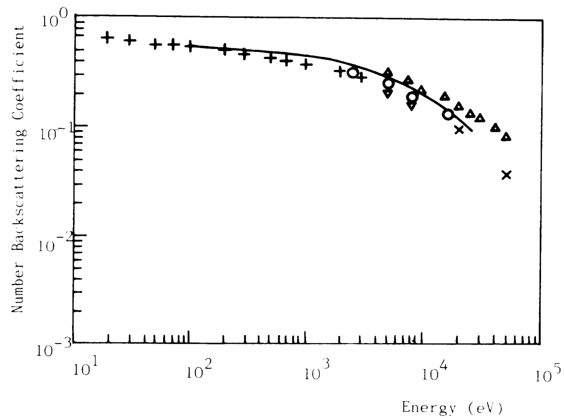

FIG. 4. Number-backscattering coefficients of H^+ ions incident on the gold target as a function of incident energy. —— denotes our computational result. ○, Eckstein and Verbeek (Ref. 25); △, Sidenius and Lenskjaer (Ref. 26); □, Sørensen (Ref. 27); △, Verbeek *et al.* (Ref. 28); ×, Eckstein and Biersack (Ref. 29); +, Eckstein and Verbeek (Ref. 25).

puters. In other words, it is far more economical than the Monte Carlo method. In order to make a direct comparison of the model with the Monte Carlo method, we have used the Monte Carlo program TCIS, an improved code of the Monte Carlo TRIM program. When using a FACOM-M 340-S computer at the computer center at Sichuan University for calculating the same problem of ion transport, for example, an ion beam of 1 keV is normally incident to Si, their CPU times are, respectively, 8 s for the bipartition model and 850 s for the TCIS program.[30] To ensure the statistical precision, we require that the number of samples is 5000. This requirement is not too rigorous. Therefore the comparison shows that the computational efficiency of the bipartition model is about 100 times higher than the Monte Carlo method.

Briefly, in the present paper we have shown that the bipartition model has successfully treated the transport problems of light ions in solids. Its precision is not lower than that of standard transport theory, yet it is capable of treating many important problems on ion injection for which the standard transport theory is invalid. Compared with the Monte Carlo method, it has much higher computational efficiency which makes its possible to link a microcomputer with an experimental facility as a high-speed analyzing system. In order to develop the potential of the bipartition model, we plan to deal with the transport problems of the ions with arbitrary atomic weight in a future article.[31]

ACKNOWLEDGMENTS

The authors wish to thank Professor Heng-De Lee, Professor De-Ping Lee, Professor Gui-Ling Liu, Professor Li-Bin Lin, and Professor Xiao-Zhong Zhang for their support. This work is part of a research program the authors submitted to the Material Science Branch of the National Science Foundation of China. Their financial support for the research is thankfully acknowledged.

APPENDIX

Let us give a proof of the formula (25). From the recurrent formula of Legendre polynomials, we have

$$\mu P'_{l+1}(\mu)-P'_l(\mu)=(l+1)P_{l+1}(\mu)\ , \tag{A1}$$

$$P'_{l+1}(\mu)-\mu P'_l(\mu)=(l+1)P_l(\mu)\ . \tag{A2}$$

Therefore

$$P_l(\mu)-P_{l+1}(\mu)=(1-\mu)[P'_{l+1}(\mu)+P'_l(\mu)]/(l+1)\ . \tag{A3}$$

Thus

$$\int_{-1}^{1}[P_l(\mu)-P_{l+1}(\mu)](1-\mu)^{-m_\lambda-1}d\mu=[P_l(\mu)+P_{l+1}(\mu)](l+1)^{-1}(1-\mu)^{-m_\lambda}\Big|_{-1}^{1} -m_\lambda(l+1)^{-1}\int_{-1}^{1}[P_l(\mu)+P_{l+1}(\mu)](1-\mu)^{-m_\lambda-1}d\mu \tag{A4}$$

and

$$\int_{-1}^{1}[1-m_\lambda(l+1)^{-1}][1-P_{l+1}(\mu)](1-\mu)^{-m_\lambda-1}d\mu=2^{1-m_\lambda}(l+1)^{-1} +\int_{-1}^{1}[1+m_\lambda(l+1)^{-1}][1-P_l(\mu)](1-\mu)^{-m_\lambda-1}d\mu\ . \tag{A5}$$

Then, we have

$$(l+1-m_\lambda)\eta_{l+1}-(l+1+m_\lambda)\eta_l-4\pi 2^{-m_\lambda}=0\ . \tag{25}$$

[1]J. R. Anderson and J. F. Gibbons, Appl. Phys. Lett. **28**, 184 (1976).
[2]L. A. Christel, J. F. Gibbons, and S. Mylroie, J. Appl. Phys. **51**, 6176 (1980).
[3]T. J. Hoffman *et al.*, Nucl. Sci. Eng. **68**, 204 (1978).
[4]J. Lindhard *et al.*, Dan. Vidensk. Selsk. Mat.-Fys. Medd. **33**, No. 10 (1963).
[5]J. B. Sanders, Can. J. Phys., **46**, 455 (1968).
[6]K. B. Winterbon *et al.*, K. Dan. Vidensk Selsk. Mat.-Fys. Medd., **37**, No. 14 (1970).
[7]D. K. Brice and K. B. Winterbon, *Ion Implantation Range and Energy Deposition Distribution* (IFL/Plenum Data, New York,

1975).

[8]J. Lindhard, M. Scharff, and H. E. Schiøtt, K. Dan. Vidensk Selsk. Mat.-Fys. Medd., **33**, No. 14 (1963).

[9]W. D. Wilson, L. G. Haggmark, and P. J. Biersack, Phys. Rev. B **15**, 2458 (1977).

[10]U. Littmark and J. F. Ziegler, Phys. Rev. A **23**, 64 (1981).

[11]H. H. Andersen and J. F. Ziegler, in *Hydrogen Stopping Power and Ranges in All Elements,* edited by J. F. Ziegler (Pergamon, New York, 1977), Vol. 3.

[12]J. F. Ziegler, Nucl. Instrum. Methods **168**, 17 (1980).

[13]Xia Yue-yuan and Tan Chun-yu, Nucl. Instrum. Methods B **13**, 100 (1986).

[14]A. R. Mitchell, *Computational Methods in Partial Differential Equations* (Wiley, New York, 1969), p. 169.

[15]J. Böttiger *et al.*, Radiat. Eff. **11**, 69 (1971).

[16]U. Littmark and A. Gras-Marti, Appl. Phys. **16**, 247 (1978).

[17]J. C. Mark, Natural Resource Council of Canada Report No. MT-92, 1944 (unpublished); MT-97, 1945 (unpublished).

[18]R. E. Marshak, Phys. Rev. **71**, 443 (1947).

[19]Luo Zhengming and Wang Shiming Nucl. Instrum. Methods (to be published).

[20]F. J. Demond *et al.*, Nucl. Instrum. Methods **168**, 69 (1980).

[21]W. K. Chu *et al.*, Phys. Rev. B **16**, 3851 (1977).

[22]E. Ligeon and A. Guivarc'h, Radiat. Eff. **27**, 129 (1976).

[23]A. Marcinkowski *et al.*, Nucl. Instrum. Methods **57**, 338 (1967).

[24]T. Tabata *et al.*, Nucl. Instrum. Methods. B **9**, 113 (1985).

[25]W. Eckstein and H. Verbeek, Max-Planck-Institut für Plasma Physik Report No. IPP9/32, 1979 (unpublished).

[26]G. Sidenius and T. Lenskjaer, Nucl. Instrum. Methods **132**, 673 (1976).

[27]H. Sørensen, *Proceedings of an International Plasma Wall Interaction,* Jülich, 1976 (Pergamon, Oxford, 1977), p. 437.

[28]H. Verbeek *et al.*, J. Appl. Phys. **51**, 1783 (1980).

[29]W. Eckstein and J. P. Biersack, Z. Phys. A **310**, 1 (1983).

[30]Cui Fuzai and Li Hengde, Nucl. Instrum. Methods B **7/8**, 650 (1985).

[31]Luo Zhengming (unpublished).